Title

Simple microscope using a compound refractive lens and a wide-bandwidth thermal neutron beam

Authors

Cremer, J. T.
Park, H.
Piestrup, M. A.
et al.

Publication Date

2007-04-06

Peer reviewed

Simple microscope using a compound refractive lens and a wide-bandwidth thermal neutron beam

J. T. Cremer,[a] H. Park, M. A. Piestrup, and C. K. Gary
Adelphi Technology Inc., 981-B Industrial Rd., San Carlos, California 94070

R. H. Pantell
Department of Electrical Engineering, Stanford University, Stanford, California 94305

R. G. Flocchini, H. P. Egbert, M. D. Kloh, and R. B. Walker
Davis McClellan Nuclear Radiation Center, University of California, McClellan, California 95652

(Received 6 November 2006; accepted 2 March 2007; published online 6 April 2007)

The results of imaging experiments using biconcave, spherical compound refractive lenses (CRLs) and a wide-bandwidth thermal neutron beam are presented. Two CRLs were used, consisting of 155 beryllium and 120 copper lenses. The experiments were performed using a thermal neutron beam line at McClellan Nuclear Radiation Center reactor. The authors obtained micrographs of cadmium slits with up to 5× magnification and 0.3 mm resolution. The CRL resolution was superior to a pinhole camera with the same aperture diameter. The modulation transfer function (MTF) of the CRL was calculated and compared with the measured MTF at five spatial frequencies, showing good agreement. © *2007 American Institute of Physics*. [DOI: 10.1063/1.2719155]

Previously, compound refractive lenses (CRLs) have been used in simple microscopes using narrow-bandwidth, cold neutrons.[1–4] We demonstrated imaging with CRLs using a wide-bandwidth ("pink") thermal neutron beam. The microscope resolution was measured by imaging periodic Cd slits to obtain the measured modulation transfer function (MTF), which closely matched the calculated MTF, which were better than predicted by geometric optics, and indicated chromatic aberration is mitigated by spherical aberration and absorption in biconcave, spherical lens CRLs. These CRLs appear to image objects with the broadband thermal neutrons as readily as an optical lens images objects in white light.

The CRL is a stack of N lenses whose total focal length $f=f_1/N$, where f_1 is the focal length of a unit lens. The CRL index of refraction $n=1-\delta+i(\lambda/4\pi)\mu$ determines the neutron refractive and attenuation properties, and depends on wavelength λ, atom density ρ, bound coherent scattering length b, decrement $\delta=\lambda^2 b\rho/2\pi$, and linear attenuation coefficient μ for absorption, incoherent scatter, and inelastic coherent scatter,[4–7] such that $\mu\propto\lambda$. Like an ordinary optical lens, the CRL can be used for imaging by placing it between an illuminated object and a detector. The lens formula, $1/f=1/o+1/i$, applies to the CRL, with distance o between object and CRL center, distance i between CRL center and detector, and magnification is $M=i/o$.

The CRL consists of N biconcave lenses, and acts as a cylinder of length l and aperture diameter $2r_e$, with limited angular acceptance $2r_e/l$ and numerical aperture r_e/f. If $f\gg l$, a neutron ray, passing through a thin lens CRL, changes direction, but not its radial distance r from the CRL center axis,[8] provided each individual lens surface has a radius of curvature R much larger than the lens thickness, $t(r)\ll R$ for $0<r<r_e$.[9] The thickness $t(r)$ of each biconcave lens increases with r from minimum, center thickness d.

For an N-lens CRL, the neutron transmission fraction $T(r)=\exp(-tN\mu)$ decreases with radial distance r from its center axis value, $T(0)=\exp(-N\mu d)$. Absorption can limit the CRL effective aperture radius r_e, which is the minimum of the CRL physical aperture radius r_m and absorption aperture radius r_a, where $r_e=\mathrm{Min}(r_m,r_a)$, such that $T(r_a)=T(0)/e^2$ and $t(r_a)=d+(2/N\mu)$. With respect to the lens midplane, the left $(-)$ and right $(+)$ lens surfaces are defined by lens half-thickness, $\tau(r)=\pm t(r)/2$. The slope of the line tangent to a lens surface at r is $dr/d\tau$, and hence the slope of the perpendicular line (normal) is $-d\tau/dr$.

A neutron ray is refracted at a lens surface by angle $\Delta\theta$ toward the lens center axis, from angle θ_1 to angle θ_2 with respect to the lens surface normal at radius r, where $\theta_2=\theta_1+\Delta\theta$ and $\Delta\theta\ll 1$. Snell's law gives $\sin\theta_1=(1-\delta)\sin(\theta_1+\Delta\theta)$ and $(1-\delta)\sin\theta_1=\sin(\theta_1+\Delta\theta)$ at the left and right lens surfaces; each causes ray angular deviation $\Delta\theta=\delta\tan\theta_1$ toward the axis with $1-\delta\cong 1$. An incident, parallel ray at r is refracted and intersects the axis at focal distance $f_1=r/2\Delta\theta$, and for an N-lens CRL the focal distance is $f=r/2N\Delta\theta$, where $\tan\theta_1=-d\tau/dr$, so that $\Delta\theta=-\delta\cdot d\tau/dr$.

A lens is between a pair of object and image points, lying on its center axis, at distances o_1 and i_1. Between the points an on-axis ray travels distance o_1+i_1, whereas an off-axis ray travels an additional distance $r^2/2o_1+r^2/2i_1$. The neutron phase velocity is slower for air/vacuum than a lens, whose thickness $t(r)$ varies to provide equal time of flight for all ray paths, where $r^2/2o_1+r^2/2i_1=t\delta$. A parabolic lens has thickness $t_p=d+(r^2/R)$ for on-axis radius of curvature R, where $R/2$ is the parabola vertex to directrix distance. With $t=t_p-d$ one obtains the lens equation $1/o_1+1/i_1=2\delta/R$, where $1/f_1=2\delta/R$. The focal length of the parabolic lens CRL is $f=R/2N\delta$, via $\Delta\theta=-r\delta/R$, and at its absorption aperture radius $r_{\mathrm{ap}}=\sqrt{2R/\mu N}$, the transmission is e^{-2} of the center axis.

A spherical lens with radius of curvature R has thickness $t_s(r)=d+2R-2\sqrt{R^2-r^2}$. The focal length of the spherical lens CRL is $f_{\mathrm{sp}}=\sqrt{R^2-r^2}/2N\delta$, via $\Delta\theta=\delta r/\sqrt{R^2-r^2}$, and its absorption aperture radius is $r_a=r_{\mathrm{ap}}\sqrt{1-(r_{\mathrm{ap}}/2R)^2}$. Spherical aberration occurs outside the center, parabolic portion of a spherical lens, and cause loss of image resolution, but not image intensity. At r the additional lens thickness Δt encoun-

[a]FAX: 650-598-9400; electronic mail: ted@adelphitech.com

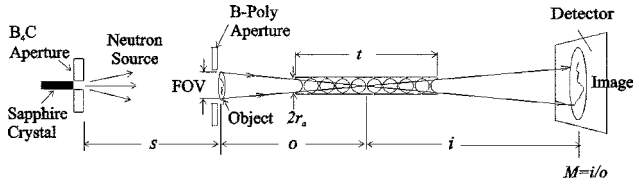

FIG. 1. Neutron microscope setup at UC Davis MNRC.

tered by neutrons propagating in the spherical lens, compared to a parabolic lens, is $\Delta t = t_s - t_p = r^4/4R^3$, and causes phase shift $\Delta\phi = 2\pi\Delta t\delta/\lambda$. Ray paths inside the parabolic aperture radius $r_p = (2R^3\lambda/N\delta)^{1/4}$ of the spherical lens CRL incur phase shift differences $\Delta\phi \leqslant \pi$, so that intensities sum at parabolic focal length $f = R/2N\delta$. Outer rays at $r > r_p$ have a spherical focal length f_{sp}, which decreases with r.

Derived with geometric optics, and neglecting interactions between absorption, spherical, and chromatic aberrations, the spherical lens CRL object resolution $\sigma_{tot}(\mu m)$ is $\sigma_{tot} = \sqrt{\sigma_R^2 + \sigma_c^2 + \sigma_{sp}^2 + \sigma_{od}^2}$. The diffraction-limited object resolution is $\sigma_R = 0.61\lambda o/r_e$, and detector limited resolution is $\sigma_{od} = \sigma_{id}/M$ for a pixel [full width at half maximum (FWHM)] width σ_{id}. Object resolution contributions from spherical σ_{sp} and chromatic aberrations σ_c are $\sigma_{sp} = \sigma r_p(r_e - r_p)/(R^2 - r_p^2)$ and $\sigma_c = 2\sigma(\Delta\lambda/\lambda)$, where $\sigma = r_e(1+M)/M$, are derived as follows. A parallel ray from the object is refracted by a spherical lens, and crosses the lens axis at its focal point, forming two similar triangles between the lens and image plane, so $y = (xi/f_{sp}) - x$ or $\Delta y = x(M+1)(-\Delta f_{sp}/f_{sp})$ with $i = (M+1)f_{sp}$, for image radius y and fixed object radius x. Varying λ for fixed r in Δf_{sp} gives σ_c and varying r for fixed λ in Δf_{sp} gives σ_{sp}.

A theoretical analysis, based on the Huygens and Fresnel's approach, used the Kirchhoff equation[7] and a 40 °C Maxwell-Boltzmann distributed source of thermal neutrons with 1.1 Å peak wavelength and 74% bandwidth FWHM, assumed for the McClellan Nuclear Radiation Center (MNRC), bay 4 beamline. From the Kirchoff equation, which accounts for both monochromatic and chromatic aberrations, we calculated the CRL point spread function (PSF) and the MTF.[9]

The MTF is a quantitative and standard measure of image quality and resolution, and describes the ability of a lens or system to transfer object contrast to the image. The resolution of a microscope generally means the capability to distinguish two point objects of about equal intensity. In the Rayleigh criterion the PSF center maximum of a second point is placed at the zero intensity position of the PSF of the first point. The Rayleigh resolution is the reciprocal of the spatial frequency s or period $1/s$ corresponding to MTF=0.09. However, the period $1/s$ at MTF=0.05 is a common resolution limit. Contrast is defined by $C = (\max - \min)/(\max + \min)$ for maximum and minimum transmitted intensities, max and min. The $\mathrm{MTF}(s) = C_i/C_o$ for image contrast $C_i(s)$ and object contrast $C_o(s)$.[9]

The experimental apparatus was installed at a thermal neutron beam line (bay 4) at the MNRC reactor. In Fig. 1, the installed apparatus consisted of a 5.7 m long optical rail, supported on a welded Al beam table, tilted at 20° relative to the floor, and aligned with the axis of the neutron beam port. Mounted to the rail was the microscope: iris and object holder, CRL, and Fuji Film[10] neutron imaging plate, an integrating detector with high detective quantum efficiency (DQE), 50 μm pixels, and 5 orders of dynamic range.

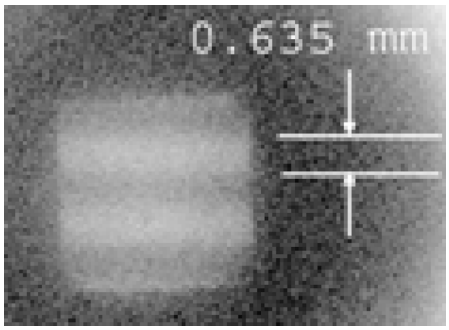

FIG. 2. Be CRL neutron image of 0.64 mm wide cadmium slits at magnification of 4.7× and wavelength λ=2.6 Å for 1 h exposure.

The thermal neutrons emerge from the reactor water core, entering the bay 4 beam tube through a graphite (moderator) end plug, and pass through a 28 cm long sapphire crystal, which improves the thermal content by reducing the relative number of higher energy neutrons. The neutrons emerge from a 3.2 cm square source aperture in a boron carbide plate, and travel distance $s = 4.0$ m through a collimation tube to the sample position. The sample is mounted in a 1.25 cm aperture, matched to the CRL field of view (FOV), of a 2.54 cm thick plate of enriched Li-polyethylene. This aperture reduces unwanted neutrons peripheral to the CRL FOV, which can scatter and decrease the image contrast and resolution. At the sample is a collimated beam (6.3 mrad divergence angle) with thermal neutron flux of 1.7×10^6 n/cm^2 s. Depending on the desired wavelength, the sample to CRL distance o is 1–2 m, and the CRL to detector distance i is 1–4 m.

To set up the microscope, we established the object o and image i distances, using the calculated CRL's focal length f and the lens equation. This was done for a particular wavelength (e.g., 2.6 Å), expected in the 40 °C Maxwell-Boltzmann MNRC thermal neutron spectrum. We positioned the Fuji Film detector, CRL, and Cd object grid using these values of o and i. Images were obtained using the Fuji Film detector, and the software package, DYNAMIX IMAGE SHARE VIEWER,[10] was used to display the images.

The CRLs are comprised of a stack of biconcave, spherical lenses, which are fabricated with inexpensive, compression-molding techniques. The Cu CRL has $N = 120$ lenses, each with radius of curvature $R = 2.0$ mm, physical aperture diameter $2r_m = 2.3$ mm, and center thickness $d = 76$ μm. The Be CRL has $N = 155$ lenses, each with radius of curvature $R = 1.9$ mm, physical aperture diameter $2r_m = 2.3$ mm, and center thickness $d = 40$ μm. Thermal neutron imaging results were obtained with the Be and Cu CRLs, and Fig. 2 shows a neutron image of 0.64 mm wide Cd slits at 4.7× magnification and 1 h exposure, produced by the Be CRL, with focal length $f = 60$ cm at $\lambda = 2.6$ Å.

To measure the MTF for the Be and Cu CRLs, we used five periodic Cd slit arrays with spatial periods of 0.5, 0.8, 1.3, 2.5, and 5.1 mm, where the slit widths were equal to the spacing between the slits. The Cd slit array acted as a periodic square wave structure with an object contrast $C_o(s) = 1$. The measured $\mathrm{MTF}(s)$ for 5 spatial periods $1/s$ was obtained from the measured image contrast $C_i(s)$. Intensity cuts perpendicular to the slit pattern were done with line-scan software, Dynamix viewer.[10] Figure 3 shows calculated MTF

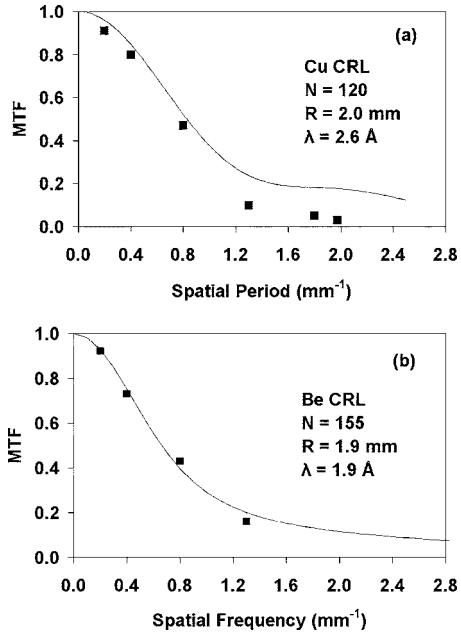

FIG. 3. The calculated and measured MTF vs spatial frequency of the slit array using (a) the Cu CRL at 2.6 Å and (b) the Be CRL at 1.9 Å.

curves and measured MTF points for the Cu CRL at 2.6 Å and Be CRL at 1.9 Å, each at ×2 magnification and 1 h exposure (6.1×10^9 n/cm^2 fluence). Based on MTF=0.05, the calculated and measured resolutions for the Cu CRL at 2.6 Å in Fig. 3(a) are 0.31 mm and 0.56 mm. For the Be CRL at 1.9 Å in Fig. 3(b) the calculated and measured resolutions are both 0.28 mm.

The geometric optics derived object resolution $\sigma_{\text{tot}}=1.1$ mm yielded a larger value for both the Cu CRL and Be CRL than the above MTF measured and calculated object resolutions. Our Kirchoff analysis shows that chromatic aberration is ameliorated by spherical aberration and absorption, resulting in better resolution than expected by σ_{tot}, because the interactions between absorption, spherical, and chromatic aberration are not included in the geometric optics resolution result σ_{tot}. With increasing lens radius r, the lens thickness $t_s(r)$ increases and the transmission fraction $T(r)\propto\exp(-r^2\lambda/R)$ decreases for longer wavelength incident rays, which focus closer to the lens than those of shorter wavelengths. These shorter wavelength rays focus further from the lens given that the lens focal length $f_{\text{sp}}\propto1/\lambda^2$, but with increasing r, the focal lengths of these rays are reduced by spherical aberration via $f_{\text{sp}}\propto\sqrt{R^2-r^2}$. Decrease of focal length deviation about its mean, yields finer resolution.

We compared the Cu and Be CRLs with their equivalent "pinhole" aperture "cameras" by use of Cd irises with diameters equal to the CRL's physical aperture ($2r_m=2.3$ mm). We constructed a one-aperture or simple pinhole camera by the placement of a single Cd iris at the center of the empty CRL lens holder. Also, we used two Cd irises mounted on each end of an empty cylindrical CRL lens holder of the same length as the Cu or Be CRL. This two-aperture case or "cylinder" formed a "thick iris" that was the same length as the matching CRL. Images from the CRL microscope and the equal-aperture-size simple pinhole camera and two-pinhole (cylinder) camera were obtained, using identical exposure times, and image and object distances. Measured intensity profiles from the Cu CRL, and its equivalent one and two pinhole cameras, are compared in Fig. 4 and show that the Cu CRL image contrast and resolution are superior.

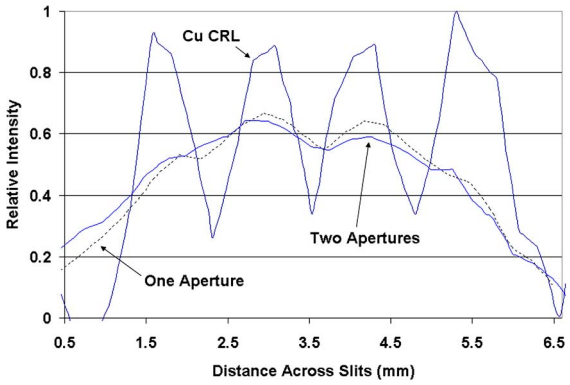

FIG. 4. Normalized image intensity vs distance across slit array (1.3 mm period) for 1-h exposure at 2.6 Å. The Cu CRL is compared with one and two aperture pinhole cameras, $o=1.7$ m and $i=3.4$ m.

The imaged Cd slits demonstrated that these CRLs were indeed acting as refractors of neutrons, and not simply as pinhole neutron cameras. For thermal wavelengths the CRL apertures are small, such that their absorption-limited aperture diameters $2r_a<2r_m$ approach the expected CRL object resolution σ_{tot}. At $\lambda=2.6$ Å and magnification $M=2$, the Cu and Be CRLs have effective aperture diameter $2r_e=2r_a=1.0$ mm and resolution $\sigma_{\text{tot}}=1.1$ mm. A pinhole camera with the same aperture diameter $2r_e=1.0$ mm has calculated object resolution $\sigma_{\text{pin}}=2r_e(M+1)/M$ or 1.5 mm. These are coarser resolutions than the range of MTF calculated and measured values of 0.28–0.56 mm.

A CRL used with a pulsed neutron source and a synchronized time of flight imaging detector[11] can improve resolution by causing the chromatic aberration to be dependent on the frame acquisition time of the detector, rather than the CRL. In a neutron pulse the neutrons arrive with steadily decreasing velocities and increasing wavelengths during the frame acquisition time. A short acquisition time Δt can result in a sufficiently small bandwidth $\Delta\lambda/\lambda=0.025$, where $\Delta\lambda\propto\Delta t$; e.g., the Be spherical lens CRL resolution could increase by 23-fold to $\sigma_{\text{tot}}=47$ μm. Spherical aberration is removed by a parabolic lens CRL.

This work was supported in part by U.S. National Institutes for Health and U.S. Department of Energy (Grant No. 1 R43 CA115248-01A1 and DE-FG02-03ER83862).

[1]M. R. Eskildsen, P. L. Gammel, E. D. Isaacs, C. Detlefs, K. Mortensen, and D. J. Bishop, Nature (London) **391**, 563 (1998).
[2]H. R. Beguiristain, I. S. Anderson, C. D. Dewhurst, M. A. Piestrup, J. T. Cremer, and R. H. Pantell, Appl. Phys. Lett. **81**, 4290 (2002).
[3]J. T. Cremer, M. A. Piestrup, C. K. Gary, R. H. Pantell, and C. J. Glinka, Appl. Phys. Lett. **85**, 494 (2004).
[4]J. T. Cremer, M. A. Piestrup, H. Park, C. K. Gary, R. H. Pantell, C. J. Glinka, and J. G. Barker, Appl. Phys. Lett. **87**, 161913 (2005).
[5]A. K. Freund, Nucl. Instrum. Methods Phys. Res. **213**, 495 (1983).
[6]V. F. Sears, J. Phys. Soc. Jpn. **65**, 1 (1996), Suppl. A.
[7]V. F. Sears, *Neutron Optics* (Oxford University Press, Oxford, 1989).
[8]R. H. Pantell, J. Feinstein, H. R. Beguiristain, M. A. Piestrup, C. K. Gary, and J. T. Cremer, Appl. Opt. **42**, 719 (2003).
[9]J. R. Meyer-Arendt, *Introduction to Classical and Modern Optics* (Prentice-Hall, Englewood Cliffs, NJ, 1984).
[10]Fuji Film Medical Systems USA, Inc., Stamford, CT 06902.
[11]R. P. Hjelm, J. Appl. Crystallogr. **21**, 618 (1988).